Neutrinos: The Key to Ultrahigh Energy Cosmic Rays

David Seckel and Todor Stanev
Bartol Research Institute, University of Delaware, Newark, Delaware 19716, USA
(Received 25 March 2005; published 29 September 2005)

Observations of ultrahigh energy cosmic rays (UHECR) do not uniquely determine both the injection spectrum and the evolution model for UHECR sources—primarily because interactions during propagation obscure the early Universe from direct observation. Detection of neutrinos produced in those same interactions, coupled with UHECR results, would provide a full description of UHECR source properties.

DOI: 10.1103/PhysRevLett.95.141101 PACS numbers: 98.70.Sa, 96.40.Tv, 98.80.Es

Ultrahigh energy cosmic rays are one of the most intriguing aspects of today's physics. Highest energy particles have long been suspected [1] to be extragalactic, because our Galaxy cannot magnetically contain, and, respectively, accelerate, them. Current experimental data on the highest energy cosmic rays show two severe problems: (1) It is equally difficult to explain their production with either traditional astrophysical acceleration models [2] or with exotic *top-down* [3] particle physics models. Acceleration models predict that UHECR are charged nuclei, whereas *top-down* models predict them to be γ rays and neutrinos. (2) Both nuclei and γ rays have small energy loss distances $\mathcal{L}_{\rm loss} = (1/E)dE/dx$. Protons of 3×10^{20} eV lose their energy in propagation on 23 Mpc. $\mathcal{L}_{\rm loss}$ declines to less than 15 Mpc at higher energy. The γ-ray energy loss distance is less certain because of the importance of the unknown isotropic radio background radiation. Reasonable estimates [4] yield about 5 Mpc at energies between 10^{19} and 10^{21} eV. Sources of UHECR then must be within several tens of Mpc, but none is identified.

The solution of these problems is also affected by the current inconsistency in the results of the two major experimental groups [5,6]. HiRes data seem to show a Greisen-Zatsepin-Kuzmin (GZK) [7] cutoff, while AGASA's UHE cosmic ray spectrum can be explained only with the addition of nearby sources or top-down scenarios.

Observations of the UHECR energy spectrum do not uniquely determine the extragalactic cosmic ray source distribution or the source spectrum even with high statistics—there are too many different ways to fit the spectrum. Figure 1 shows two extreme fits. The top panel illustrates a fit with a flat E^{-2} injection spectrum and $(1+z)^m (m = 3, 4)$ cosmological evolution of the cosmic ray sources. Such fits [8,9] can represent UHECR spectrum adequately if galactic cosmic rays extend above 10^{19} eV. Correspondingly, the chemical composition of cosmic rays contains a fraction of heavy nuclei up to that energy. In these models the second cosmic ray knee [5,6,10–12] is where extragalactic cosmic rays prevail over the galactic ones. Fits with flat injection spectra require some cosmological evolution of the UHECR sources. Note, however, that this has a small effect on UHECR above 10^{19} eV since the contributions from large redshifts are small.

A different type of fit is illustrated in the bottom panel of Fig. 1. Extragalactic cosmic rays with injection spectrum $E^{-2.7}$ prevail down to 10^{18} eV [13,14]. These cosmic rays are expected to be protons and He nuclei. Generally injection spectra steeper than $E^{-2.5}$ can fit the observed spectra without strong redshift evolution. The shape of the spectrum reflects the transition of dE/dx from pair production [15] to purely adiabatic losses. The galactic cosmic ray spectrum extends to about 10^{18} eV. The spectral shape of the extragalactic cosmic rays has to be flatter below 10^{18} eV not to contradict data. One possible explanation is the limited horizon of lower energy extragalactic cosmic rays due to scattering in extragalactic magnetic fields [16,17]. Both fits require about the same luminosity above

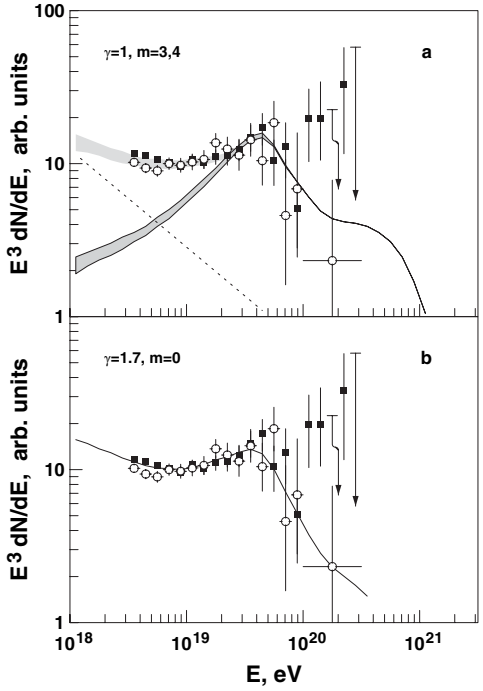

FIG. 1. (a) A fit of UHECR spectrum with flat extragalactic injection spectrum. Upper and lower edges of shaded area are for $m = 4$ and 3. Galactic contribution is (dotted line) with $\gamma = 2.6$. (b) Fitting with steep injection spectrum ($\gamma = 1.7$).

10^{19} eV, although for a steeper injection spectrum the luminosity below 10^{19} eV is significantly greater.

Cosmogenic (GZK) neutrino production.—As shown in Fig. 1, different UHE cosmic ray source models produce spectra consistent with observations. The differences at lower energy may be disguised by contributions from the galaxy, or by propagation effects. The model degeneracy can be broken by considering the neutrino flux produced by the UHECR via their interactions on the cosmic microwave background [18,19], often called the GZK neutrino flux.

To make the point, we consider a set of simple power law models in a matter dominated cosmology, with a homogeneous distribution of UHECR sources. On cosmological time scales, the UHECR interact quickly with the CMB, so we model the production of cosmogenic neutrinos as instantaneous with particle injection. We use the neutrino yields of Ref. [20]. The neutrino flux at Earth due to GZK production is

$$E_\nu \frac{d\Phi}{dE_\nu}(E_\nu) = \frac{c}{4\pi} \int dt d\epsilon_p \frac{d\Gamma}{d\epsilon_p} E_\nu \frac{dy}{dE_\nu}(E_\nu, \epsilon_p, t), \quad (1)$$

where Γ is the injection rate of UHECR, y is the neutrino yield per proton injected with energy ϵ_p, and E_ν is the neutrino energy today.

We recast Eq. (1) by defining $q = 1 + z$ and integrating over redshift. For a matter dominated cosmology, $H_0 dt = -q^{-3/2} d(\ln q)$, where H_0 is the present day Hubble parameter. As a function of redshift, we model the UHECR injection rate as

$$\frac{d\Gamma}{d\epsilon_p} = q^m \epsilon_p^{-(1+\gamma)} A, \quad (2)$$

where γ is the integral spectral index of the source, m describes the evolution of the comoving source density, and A is chosen to normalize the emissivity of UHECR sources to their energy density in the present Universe. We use $\mathcal{L}_{\rm CR} = 4.5 \times 10^{44}$ erg Mpc^{-3} yr^{-1} as estimated by Waxman [21]. The neutrino yield can also be scaled with redshift. Defining the present day yield as $\frac{dy_0}{dE_\nu}(E_\nu, E_p)$, the yield from a previous epoch is

$$E_\nu \frac{dy}{dE_\nu}(E_\nu, \epsilon_p, z) = E_\nu \frac{dy_0}{dE_\nu}(q^2 E_\nu, q\epsilon_p). \quad (3)$$

The factors of q are due to the redshift of neutrino energy from production to the current epoch, and to the lowering of the reaction threshold due to the increased CMB temperature in the early Universe. Let Y_0 be the integrated yield from injecting an $E_p^{-(1+\gamma)}$ spectrum today: $E_\nu \frac{dY_{0\gamma}}{dE_\nu}(E_\nu) = \int dE_p E_p^{-(1+\gamma)} E_\nu \frac{dy_0}{dE_\nu}(E_\nu, E_p)$. Then the integral yield at any other redshift is given by

$$\int d\epsilon_p \epsilon_p^{-(1+\gamma)} E_\nu \frac{dy}{dE_\nu}(E_\nu, \epsilon_p, t) = q^\gamma E_\nu \frac{dY_{0\gamma}}{dE_\nu}(q^2 E_\nu). \quad (4)$$

With these definitions, the GZK production integral can be expressed as an integral over redshift,

$$E_\nu \frac{d\Phi}{dE_\nu}(E_\nu) = \frac{cA}{4\pi H_0} \int_0^{q_{\rm max}} d(\ln q) q^{(m+\gamma-3/2)} \times E_\nu \frac{dY_{0\gamma}}{dE_\nu}(q^2 E_\nu). \quad (5)$$

Written as an integral over $\ln q$, it is straightforward to see which epoch dominates the neutrino flux. If $m + \gamma = 1.5$ then all redshift intervals contribute with comparable importance. This is illustrated by the top panel of Fig. 2, where $m = 0.5$, $\gamma = 1$. The thin lines represent the contribution to the neutrino flux from epochs spaced equally in $\ln q$, and of equal width in $d(\ln q)$. The peak contribution for each interval occurs at an energy $E_{\rm pk}(q)$, which scales with redshift as $E_{\rm pk}(q) = E_{\rm pk}(0)/q^2$. The sum of the thin lines, back to a redshift of $1 + z_{\rm max} = 10$, gives the dotted curve—the predicted GZK neutrino flux for the model. The integrated flux is flat, with a width in E_ν of order $(1 + z_{\rm max})^2$.

Similarly, the middle panel illustrates a second model with equal contribution per epoch, although here there is no evolution ($m = 0$) and the spectrum is correspondingly steeper ($\gamma = 1.5$). The total cosmogenic neutrino flux is reduced due to the smaller number of injected protons. The larger value of γ is evident only through the different slope of the high energy part of the neutrino spectrum. In contrast, if $m + \gamma > 1.5$ the neutrino flux is dominated by past

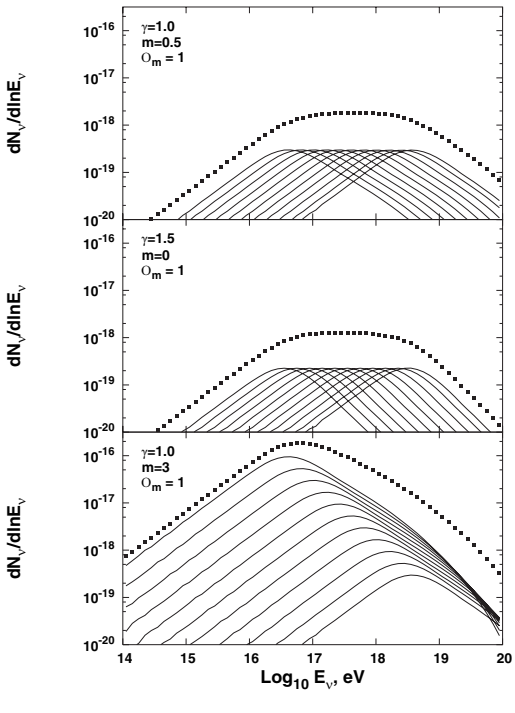

FIG. 2. Neutrino production in three simplified models for the source spectrum and evolution of UHECR. To enhance the contrast between different models, the source luminosity is extended out to $1 + z_{\rm max} = 10$.

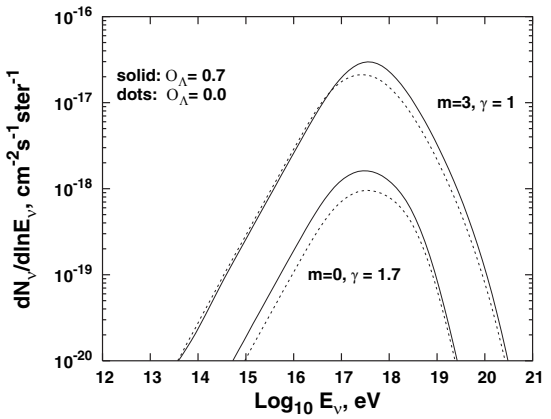

FIG. 3. Neutrino production for the UHECR models shown in Fig. 1. The injection spectrum is cut off at $E_c = 3 \times 10^{21}$ GeV, and the source evolution is that described in Ref. [20]. Model results depend mildly on the cosmological model, $\Omega_\Lambda = 0.0$ or 0.7.

epochs. The bottom panel of Fig. 2 illustrates this situation for a flat source model with significant evolution, $m = 3$, $\gamma = 1$. Note that this illustrative model is not realistic as the $(1 + z)^3$ evolution continues to $1 + z_{\max} = 10$.

Discussion.—The scaling analysis illustrates the combined importance of the UHECR spectrum and cosmological evolution in estimating the neutrino flux due to GZK production. For more realistic models, it is appropriate to consider other effects, such as a cosmological constant, a cutoff to the cosmic ray injection spectrum, and a cutoff or break in scale to the source evolution model. These effects alter the details of GZK production, but do not change the overall picture. Accordingly, Fig. 3 shows an order of magnitude difference in the GZK production for the two extreme UHECR models presented in Fig. 1. Apart from the lower value of $z_{\max}$, the steep source model with no evolution ($\gamma = 1.7$, $m = 0$) is similar to the middle panel of Fig. 2. The model with flat spectrum and cosmological evolution ($\gamma = 1$, $m = 3$) predicts an order of magnitude larger flux. Even faster evolution ($m = 4$ as shown in Fig. 1) or flatter spectra [22] could give a further increase.

This brings us to the main point of this Letter. The AUGER observatory, under construction, will measure the intensity and spectrum of UHECR. Above the GZK cutoff these are observations of the current Universe. Below the GZK cutoff it may be difficult to separate the old intergalactic cosmic rays from a population of young cosmic rays that originate within our own galaxy. Complementary to AUGER, experiments are being designed and constructed (ANITA, IceCube, Mediterranean km^3, RICE), which may confirm the existence of GZK neutrinos. A next generation of experiments (EUSO, OWL, SalSA, X-RICE) is being planned, which would provide sufficient statistics [O(100) GZK events per year] to complement and expand the AUGER observations. Successful completion of one such experiment would be an important step toward understanding the sources of the highest energy particles in the Universe.

It is often argued that neutrino astronomy has value in that neutrinos allow observation of the interior of objects, whereas photons allow only observation of the surface. Solar neutrinos are an example, confirming theoretical models of the thermonuclear furnace in the sun, by direct observation of the core. The current discussion is similar. The ''surface'' is the interaction distance for super-GZK UHECR. The ''interior'' is the early Universe, where the evolution of UHECR sources can be directly observed through the GZK neutrino flux.

This research is supported in part by NASA Grant No. NAG5-10919. T. S. is also supported by U.S. Department of Energy Contract No. DE-FG02 91ER 40626.

[1] G. Cocconi, Nuovo Cimento **3**, 1433 (1956).
[2] D. P. Torres and L. A. Anchordoqui, Rep. Prog. Phys. **67**, 1663 (2004).
[3] P. Bhattacharjee and G. Sigl, Phys. Rep. **327**, 109 (2000).
[4] R. J. Protheroe and P. L. Biermann, Astropart. Phys. **6**, 45 (1996).
[5] M. Takeda *et al.* (AGASA Collaboration), Phys. Rev. Lett. **81**, 1163 (1998); M. Takeda *et al.* (AGASA Collaboration), Astropart. Phys. **19**, 447 (2003); see also the AGASA Web page http://www-akeno.icrr.u-tokyo.ac.jp/AGASA.
[6] R. U. Abbasi *et al.* (HiRes Collaboration), Phys. Rev. Lett. **92**, 151101 (2004).
[7] K. Greisen, Phys. Rev. Lett. **16**, 748 (1966); G. T. Zatsepin and V. A. Kuzmin, JETP Lett. **4**, 78 (1966).
[8] E. Waxman and J. N. Bahcall, Phys. Lett. B **556**, 1 (2003).
[9] T. Wibig and A. W. Wolfendale, J. Phys. G **31**, 255 (2005).
[10] A. V. Glushkov *et al.* (Yakutsk Collaboration), in *Proceedings of the 28th International Cosmic Ray Conference, Tsukuba, Japan, 2003* (Universal Academy Press, Tokyo, 2003), p. 389.
[11] D. J. Bird *et al.* (HiRes Collaboration), Phys. Rev. Lett. **71**, 3401 (1993).
[12] R. U. Abbasi *et al.* (HiRes Collaboration), Astrophys. J. **622**, 910 (2005).
[13] V. S. Berezinsky, A. Z. Gazizov, and S. I. Grigorieva, hep-ph/0204357; astro-ph/0210095.
[14] V. S. Berezinsky, A. Z. Gazizov, and S. I. Grigorieva, Phys. Lett. B **612**, 147 (2005).
[15] V. S. Berezinsky and S. I. Grigorieva, Astron. Astrophys. **199**, 1 (1988).
[16] M. Lemoine, Phys. Rev. D **71**, 083007 (2005).
[17] R. Aloisio and V. S. Berezinsky, Astrophys. J. **625**, 249 (2005).
[18] V. S. Berezinsky and G. T. Zatsepin, Phys. Lett. B **28**, 423 (1969); Sov. J. Nucl. Phys. **11**, 111 (1970).
[19] F. W. Stecker, Astrophys. Space Sci. **20**, 47 (1973).
[20] R. Engel, D. Seckel, and T. Stanev, Phys. Rev. D **64**, 093010 (2001).
[21] E. Waxman, Astrophys. J. **452**, L1 (1995).
[22] O. E. Kalashev *et al.*, Phys. Rev. D **66**, 063004 (2002).